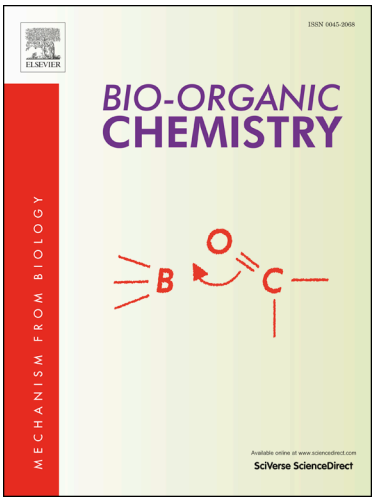

Synthesis and characterization of new inhibitors of cholinesterases based on *N*-phenylcarbamates: *In vitro* study of inhibitory effect, type of inhibition, lipophilicity and molecular docking

Katarína Vorč áková, Magdaléna Májeková, Eva Horáková, Pavel Drabina, Miloš Sedlák, Š árka Štěpánková

PII: S0045-2068(18)30020-8
DOI: https://doi.org/10.1016/j.bioorg.2018.03.012
Reference: YBIOO 2302

To appear in: *Bioorganic Chemistry*

Received Date: 9 January 2018
Revised Date: 9 March 2018
Accepted Date: 12 March 2018

Please cite this article as: K. Vorč áková, M. Májeková, E. Horáková, P. Drabina, M. Sedlák, S. Štěpánková, Synthesis and characterization of new inhibitors of cholinesterases based on *N*-phenylcarbamates: *In vitro* study of inhibitory effect, type of inhibition, lipophilicity and molecular docking, *Bioorganic Chemistry* (2018), doi: https://doi.org/10.1016/j.bioorg.2018.03.012

Synthesis and characterization of new inhibitors of cholinesterases based on *N*-phenylcarbamates: *In vitro* study of inhibitory effect, type of inhibition, lipophilicity and molecular docking

Katarína Vorčáková[1], Magdaléna Májeková[2], Eva Horáková[3], Pavel Drabina[3], Miloš Sedlák[3], Šárka Štěpánková[1,*]

[1] Department of Biological and Biochemical Sciences, Faculty of Chemical Technology, University of Pardubice, Pardubice, Czech Republic

[2] Department of Biochemical Pharmacology, Institute of Experimental Pharmacology & Toxicology, Slovak Academy of Science, Bratislava, Slovak Republic

[3] Institute of Organic Chemistry and Technology, Faculty of Chemical Technology, University of Pardubice, Pardubice, Czech Republic

[*] Corresponding author: email: sarka.stepankova@upce.cz, Studentská 573, 53210 Pardubice, Czech Republic. Telephone: +421 466 037 294, fax number: +421 466 037 068

Keywords

Carbamates; Monosaccharide derivatives; Cholinesterases; IC_{50}; Molecular Modeling; Water Bridge

Abstract

Based on current treatment of Alzheimer's disease, where the carbamate inhibitor Rivastigmine is used, two series of carbamate derivatives were prepared: i) *N*-phenylcarbamates with additional carbamate group (**1-12**) and ii) *N*-phenylcarbamates with monosaccharide moiety (**13-24**). All compounds were tested for the inhibitory effect on both of the cholinesterases, electric ell acetylcholinesterase (eeAChE) and butyrylcholinesterase from equine serum (eqBChE) and the inhibitory activity (expressed as IC_{50} values) was compared with that of the established drugs Galanthamine and Rivastigmine. The compounds with two carbamate groups **1-12** revealed higher inhibitory efficiency on both cholinesterases in compared with monosaccharide derived carbamates **13-24** and with Rivastigmine. The significant decrease of inhibitory efficiency on eqBChE (also for eeAChE but in less manner) was observed after deacetalization of monosaccharide. Moreover, the type of inhibitory mechanism of five chosen compounds was studied. It was found, that compounds with two carbamate groups act presumably via a mixed inhibitory mechanism and the compounds with monosaccharide moiety act as non-competitive inhibitors. The lipophilicity of tested compounds was determined using partition coefficient. Specific positions of the inhibitors in the binding sites of cholinesterases were determined using molecular modeling and the results indicate the importance of phenylcarbamate orientation in the catalytic gorges of both enzymes.

1. Introduction

Alzheimer's disease represent the most common type of dementia with characteristic symptoms, i.e. changes in levels of ChEs, enhanced production and accumulation of β-amyloid peptide, formation of neurofibrillary tangles inside nerve cell bodies etc. In process of development of AD, the levels of ChEs are altered in different manner. In early stages of AD, the level of AChE is increased at a much higher rate than level of BChE. On the other hand, in later stages of AD, decrease of level AChE and rapid increase of level of BChE in brain occurs. In this stage, BChE substitutes the function of AChE – the hydrolysis of acetylcholine (ACh). Generally, the inferior level of ACh during AD is obvious and therefore inhibition of ChEs represents one of the major pharmacological interventions for this disease [1].

Inhibitors of cholinesterases (ChEIs) represent a wide-range group of different chemical substances with application in two areas. The first one involves the pharmaceutical employment (as cholinergic drugs) for treatment of various diseases such as Alzheimer's disease and other dementias, Myasthenia gravis and glaucoma. The second one includes their using as pesticides or chemical warfare nerve agents [2]. Generally, carbamate inhibitors, such as Alzheimer's disease drug Rivastigmine ((*S*)-*N*-ethyl-3-[(1-dimethylamino)ethyl] *N*-methylphenylcarbamate), are classified as the pseudo-irreversible inhibitors, which form a carbamoylated complex with the serine residue of the catalytic triad [3,4]. It was found out, that Rivastigmine exhibits tenfold greater affinity for brain AChE than for the peripheral one. This selectivity for the brain enzyme and inhibitory activity against AChE and BChE makes Rivastigmine a drug with a good pharmacological profile [5]. Another member of ChEIs – Cymserine (or more potent and selective bisnorcymserine), represents a BChE selective carbamate inhibitor, which is currently pursued for clinical development as an Alzheimer

therapeutics. The structure of Cymserine was designed on the basis of the structure of the alkaloid physostigmine [6,7].

Currently, utilization of carbamate functional group incorporated to the structure of inhibitor plays an important role in modern drug discovery and medicinal chemistry. Carbamate functional group can be found in many of approved therapeutic agents, besides Rivastigmine, i.e. Felbamate (antiepileptic drug), Flupirtine (nonopioid analgesic), Albendazole (anthelmintic drug), Efavirenz (inhibitor of reverse transcriptase), Ritonavir (inhibitor of HIV-1 and HIV-2 protease) etc. [8]. Using two carbamate groups in molecule (biscarbamate) also represent a potential area. In the past, we can found using biscarbamates in synthesis antitumor compounds [9,10] and also as inhibitors of acetylcholinesterase [11]. Nowadays, group of researcher *Bosak et al.* intensively work on synthesis new biscarbamate compounds as butyrylcholinesterase inhibitors [12,13].

The compounds containing halogen atom could allow the formation of specific type of non-covalent interaction – halogen bonding – formed between a halogenated compound as inhibitor and protein backbone of cholinesterase enzymes [14–24]. There are a number of experimental studies, where the effect of halogen substitution on binding affinity has been systematically evaluated [25–27]. In some cases, present halogen atom, which enables the formation of halogen bonding, led to the significant increase of binding affinity. The explanation of this effect lays in the structure of catalytic triad of ChEs constituted from three aminoacids His-Ser-Glu, in which nitrogen atoms of histidine participate in this type of interaction. In addition, histidine can form another types of interactions, e.g. hydrogen bonds, charge−charge or charge-dipole interactions, π−π-contacts, or complexes with metal ions [19]. This fact can be also considered in designing of new ChEs inhibitors.

Furthermore, one of the most popular halogen-containing functional groups in drug molecules is the trifluoromethyl moiety (CF_3) [28]. Many of familiar drugs contain trifluoromethyl group, e.g. antidepressants (Prozac and Luvox), anaesthetics (Halothane,) or antimalarial drug Lariam [29]. *Martins et al*. published a series of trifluoromethylated isoxazoles exhibiting antimicrobial activity [30]. Finally, also several ChEs inhibitors containing CF_3 moiety were previously described [31,32].

The compounds with monosaccharide moiety could possess a high level of ability to pass through blood-brain barrier via GLUT-family sugar/polyol transport facilitators into intracellular space of CNS, what can lead to their enhanced inhibitory activity [33–36]. Moreover, monosaccharide moiety is generally used in designing of structure of new drugs in order to improve their water solubility or serum stability [34]. Phenolic glycosides can be a part of some natural products [37]. Our research group previously published the study in which *N*-(2-phenylcyclopropyl)carbamates with monosaccharide moiety were tested as potential cholinesterase inhibitors. Some of them were evaluated as quite potent in inhibition of BChE with IC_{50} in micromolar range [38].

Nowadays, many researchers are focused on studying the role of butyrylcholinesterase (as the second cholinesterase (ChE)) in human body, especially in the brain of patients with Alzheimer's disease (AD) during the process of degeneration of nerve cells. In addition, other functions of this enzyme are also investigated. With regard to the fact, that BChE is present in plasma (where its average concentration is 5 mg/L) and numerous vertebrate tissues (liver, intestine and lung), some studies discuss the noncholinergic functions of BChE in detoxification of numerous drugs and toxins [39,40]. For example, purified BChE was used for treatment of succinylcholine-induced apnea in humans. Further, it is known that BChE to protect rodents from the toxic effects of cocaine [41,42]. The therapeutic potential of BChE

relies on its ability to stay in the circulation for a prolonged period, which in turn depends on maintaining its tetrameric quaternary configuration. BChE occured in the neuromuscular junctions and the central nervous system is anchored to membranes via interactions with ColQ (AChE-associated collagen tail protein) and PRiMA (proline-rich membrane anchor) proteins containing proline-rich domains [43,44].

The above-mentioned findings inspired us for synthesis and characterization of twenty-four differently substituted *N*-phenylcarbamates, whose inhibitory activity against ChEs and lipophility should be evaluated. In the case of the most promising compounds, we also focused on study of mechanism of inhibitory effect using the molecular modeling.

2. Results and discussion

2.1 Chemistry

The preparation of target carbamate derivatives **1-12** was performed by two-step synthesis described previously (Scheme 1). The synthesis started from 3-aminophenol as the structural core of all carbamates **1-12**. It was transformed to corresponding *N*-(3-hydroxyphenyl)carbamates by the action of methyl, ethyl or butyl chloroformate. Two equivalents of 3-aminophenol were used with regard to the formation of its unreactive hydrochloride during the reaction course. The application of different bases, e.g. triethylamine, led to undesired by-products and less yields of the reaction, caused by formation of phenolate anion in equilibrium and subsequent O-acylation. The yields of this first step were satisfactory (50–75%). The structure of these monocarbamate intermediates was confirmed by means of ^{1}H NMR spectroscopy. The second reaction step included the formation of further carbamate group by the addition of *N*-(3-hydroxyphenyl)carbamates into slight excess of phenyl isocyanate derivatives in the presence of triethylamine as base catalyst. Beside non-substituted, 4-methylphenyl and 4-methoxyphenyl isocyanate also 4-

chlorophenyl and 3,4-dichlorophenyl derivatives were chosen, based on above mentioned data in introduction. The urea possibly formed as a by-product was removed by purification of products by means of column chromatography. Yields of these transformations were almost quantitative [45].

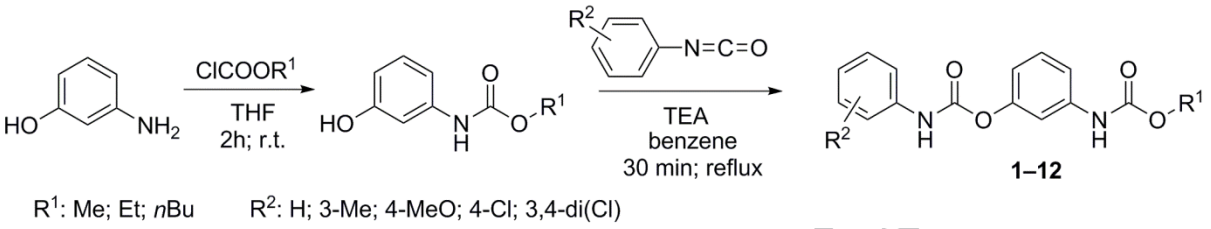

Scheme 1. Preparation of *N*-phenylcarbamate derivatives **1–12** (*The first group*).

The second group of studied carbamate derivatives **13–24** contained monosaccharide moiety in their structure. The preparation of carbamates **13–18** was performed by simple treatment of the protected monosaccharide with corresponding phenyl isocyanates (Scheme 2). This addition reaction was catalyzed by triethylamine. In this case, the reaction needed high temperature (reflux in 1,4-dioxane) and relatively long reaction time to achieve satisfactory yields (31–67%). Unreacted monosaccharide as well as isocyanate was removed by means of column chromatography. Furthermore, the group of carbamate derivatives **19–24** was obtained by deprotection of compounds **13–18** (deacetalization of monosaccharide moiety) performed in aqueous trifluoroacetic acid (TFA) (1/1) [46]. The deprotection proceeded with high conversion at set condition (24 h, r.t.). The products were obtained as a mixture of both anomers, which were detected in NMR spectra as two sets of signals. Completion of deprotection process can be monitored by means of ^{1}H NMR spectroscopy as marked disappearing of characteristic signals of methyls belonging to protecting groups in area 1.30–1.60 ppm. All carbamates **13-24** were characterized by melting point, ^{1}H and ^{13}C NMR spectroscopy and high resolution mass spectroscopy.

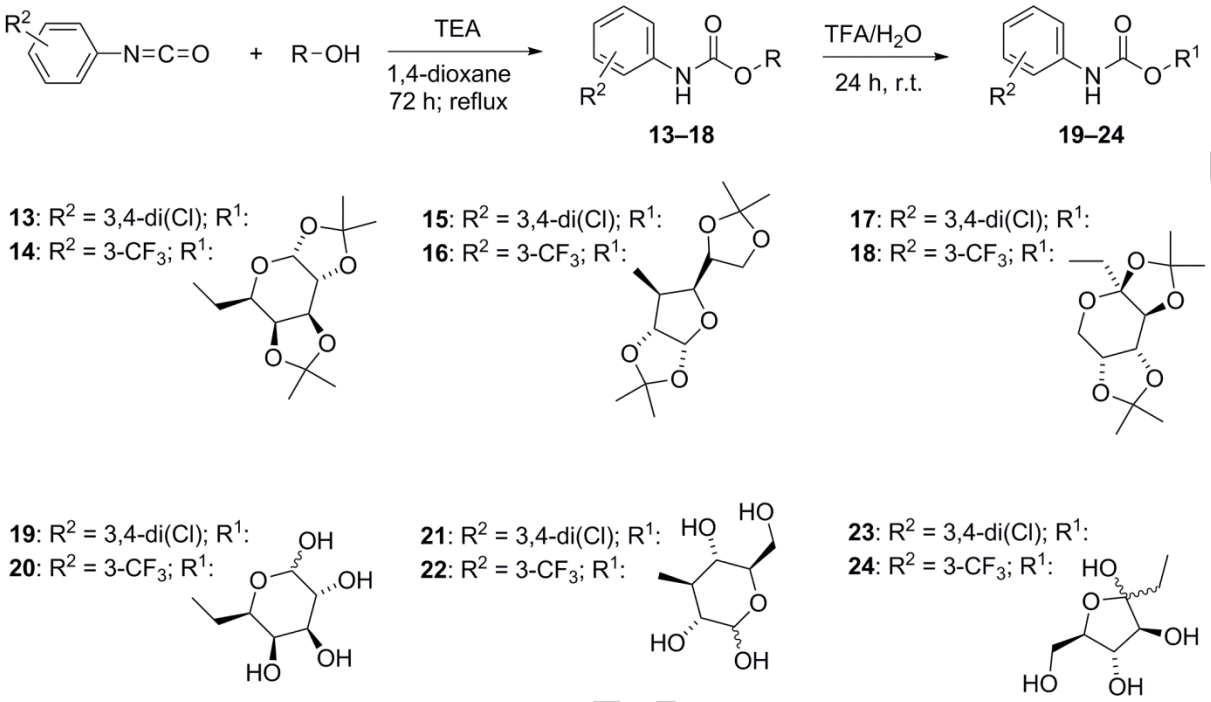

Scheme 2. Preparation of *N*-phenylcarbamate derivatives **13–24** (*The second group*).

2.2 In vitro acetylcholinesterase and butyrylcholinesterase inhibition

The ability of the investigated *N*-phenylcarbamate derivatives **1–24** to inhibit eeAChE and eqBChE was screened *in vitro* using modified Ellman's method. The effectiveness of the inhibitors is expressed as IC_{50}, representing the concentration of an inhibitor required for 50% inhibition of the enzyme. The obtained results were compared with those obtained for Rivastigmine (acylating pseudo-irreversible carbamate inhibitor that inhibits AChE as well as BChE) and Galanthamine (non-acylating competitive reversible inhibitor) (Table 1).

Tab. 1

The first group of tested substituted *N*-phenylcarbamates **1-12** represents moderate or quite potent inhibitors on both of cholinesterases what correlate with results from molecular modeling. This group of inhibitors shows more inhibition potency for eqBChE. The values of IC_{50} are in the range from 7.7 to 20.9 µM for eeAChE and from 6.1 to 22.0 µM for eqBChE.

In general, it is possible to conclude that better effectiveness was achieved when the halogen substitution (chloro) was present. Inhibitors with two atoms of chlorine (*N*-3,4-dichlorophenyl derivatives **10**-**12**) have lower values of IC_{50} and were identified as more effective eqBChE (also eeAChE) inhibitors in contrast with compounds without chlorine.

The second group of tested substituted *N*-phenylcarbamates **13-24** exhibits inhibition efficiency in wide range for both ChEs and significant difference between protected monosaccharide derivatives and their deprotected version is also obvious. For eeAChE is the range of inhibitory concentration from 46.9 to 103.5 μM and the inhibitors with protected monosaccharide moiety have inhibitory concentration approximately two times lower as the inhibitors with deprotected monosaccharide moiety. In case of eqBChE, for the compounds **13**, **14**, **17** and **18** the lower inhibitory concentration in comparison of eeAChE was observed. The other compounds from this group possessed very low inhibitory activity (> 200 μM). In some cases, the introduction of CF_3 group into phenol slightly increases IC_{50} values for both ChEs.

The inhibitory activities of *N*-phenylcarbamate derivatives **1-24** were compared with those of Galanthamine and Rivastigmine. All of the tested compounds **1-24** showed a worse inhibition of eeAChE and eqBChE than Galanthamine. The first group of tested compounds **1-12** exhibited better inhibition efficiency for both of ChEs in comparison with Rivastigmine. In case of the second group of tested compounds **13-24**, the higher inhibitory concentration for eeAChE was determined. For eqBChE only the compounds **13**, **14**, **17** and **18** had lower inhibitory concentration in comparison of Rivastigmine.

Considering the selectivity for AChE *vs.* BChE (see Tab. 1) all tested compounds (except **15-17** and **19-24**) showed a balanced inhibition of both ChEs (AChE/BChE ratio <2).

The kinetic parameters K_m and V_m for tested compounds **1**, **10**, **12**, **13** and **18** were calculated from the Lineweaver-Burk plot and based on results the type of inhibition was evaluated. The kinetic parameters, for reactions in the presence of the tested compounds **1**, **10** and **12**, were changed in different extent compared to the value for the reaction in their absence. These results indicated that group of inhibitors **1-12** inhibits BChE in a varied manner and it could be concluded that this group of compounds presumably acts via a mixed inhibitory mechanism. On the other hand, the compounds with monosaccharide moiety **13-18**, presumably act via a non-competitive inhibitory mechanism. The V_m values obtained for the inhibited reactions were lower than V_m for the reaction in the absence of the inhibitor, the K_m values did not change in the presence or absence of the inhibitor. The example of kinetic analysis for compound **18** is shown in Figure 1.

Fig. 1

2.3 Partition coefficient

The ability of tested inhibitors to pass across the blood-brain barrier (BBB) was estimated by traditional shake-flask method. The optimal values of partition coefficient are in range 4-5. This property of compounds represents better transport of the active molecules into intracellular space of CNS. The results of partition coefficient are presented in Table 1. Almost all of tested compounds have value of partition coefficient in range 3.3-6.32 (except **15**, **19-24**). Compounds with deprotected monosaccharide moiety had the values of partition coefficient lower than 3.1, as the result of deacetalization of monosaccharide moiety when the compounds became more hydrophilic.

2.4 Molecular modeling

The compounds studied are poor to moderate inhibitors of both AChE and BChE, with the exception of compounds **10**, **11** and **12**. For this reason we concentrated our *in silico* study on these derivatives. Compound **10**, the most effective inhibitor of both enzymes, is firmly set in the active site of BChE by H-bond with His438 and water mediated H-bond with Ser198, two members of the catalytic triad Ser198, Glu325 and His338. The position is further stabilized by π-π interaction of the phenyl group with His438, H-bond with Tyr440 and hydrophobic interaction with Gly117 (Figure 2A, left). The whole complex is fixed by a compact water network over di-Cl-phenyl part of molecule as it can be easy visible from the space over the gorge of BChE (Figure 2A, right). Changing methyl substituted phenylcarbamate moiety by sugar (α-D-galactopyranose) in compound **19** caused turning of the whole molecule (probably due changing the orientation of a lipole – a lipophilic dipole) out of the position obtained for compound **10**. The sugar moiety is kept by Glu197 and Gly115 and water does not create a systematic network as for compound **10**. No interaction with the member of catalytic triad was observed (Figure 2B).

Fig. 2

A similar situation as for BChE was found for compound **10** in AChE, however, in this case compound **10** interacts with Ser203 of the catalytic triad and the gap to the active site is narrower (Figure 3).

Fig. 3

3. Conclusions

A series of twenty-four *N*-phenylcarbamates **1-24** were evaluated for their inhibition against AChE from electric eel and BChE from equine serum. Inhibitory concentration was in micromolar range. It was observed that derivatives containing chlorine atoms possess higher inhibitory efficiency. On the other hand, the substitution of benzene ring by CF_3 increases the

inhibitory concentration. The compounds with monosaccharide moiety **13-24** showed lower inhibitory efficiency in comparison with compounds with two carbamate groups **1-12**. This fact is probably related to recently observed trend of molecules with higher number of OH groups to behave as PAINS (the compounds giving moderate or poor interactions with many proteins, through manifold OH-mediated H-bonds). Such interactions result in a poor enzyme selectivity, therefore the compounds **13-24** do not act as selective inhibitors of AChE and BChE.

Based on results of type of inhibition, the compounds **1-12** presumably belong to the group of inhibitors with mixed type of inhibition and the compounds **13-24** presumably act as non-competitive inhibitors. Owing to the obtained results of partition coefficient, it is possible to conclude that all of the tested phenylcarbamates should pass across the blood-brain barrier.

4. Materials and methods

4.1 Chemistry

4.1.1 General

All reagents and solvents were purchased from Penta Chemicals or Sigma Aldrich. The starting chemicals (including phenyl, 3-methylphenyl, 4-methoxyphenyl, 4-chlorophenyl, 3,4-dichlorophenyl and 3-trifluoromethylphenyl isocyanate) were obtained from Sigma-Aldrich or TCI Chemicals and used without further purification. The synthetic method for preparation of compounds **1-12** was published by *Bergon et al.* [47]. The compounds **1–4** and **8–11** were described by *Boroschewski et al.* [48], purity and characterization data were verified.

Column chromatography was performed using 60 Å (60–200 μm) silica gel. All solvents were reagent-grade and when necessary, were purified and dried by standard methods. TLC was performed on aluminium-backed silica gel plates (Merck DC, Alufolien Kieselgel 60 F_{254}) with spots visualized by UV light. The melting point temperatures are uncorrected. FT-IR spectra were measured on a Nicolet iS50 instrument. ^{1}H NMR spectra were recorded on a

Bruker Avance 400 instrument. Chemical shifts δ were referenced to the residual peak of the $CDCl_3$ at 7.26 ppm. The ^{13}C NMR spectra were calibrated with respect to the middle signal in the triplet of $CDCl_3$ (δ = 77.23 ppm) or the multiplet of CD_3OD (δ = 49.00 ppm) and DMSO-d_6 (δ = 39.51 ppm). High-resolution mass spectra were measured on the Thermo Fisher Scientific MALDI LTQ Orbitrap instrument. The used matrix was 0.2M solution of 2,5-dihydroxybenzoic acid (DHB) in MeCN/H_2O (95/5). Spectra were calibrated with respect to used matrix.

4.1.2 Synthesis of compounds

4.1.2.1 Synthesis of substituted carbamates **1–12** [47]

The carbamates **1–12** were prepared by a two-steps process. Methyl, ethyl or butyl chloroformate (0.025 mol) was added dropwise to 3-aminophenol (0.05 mol) dissolved in dry THF (50 mL) at room temperature. The mixture was stirred for 2 h and the hydrochloride of 3-aminophenol formed was filtered off. The filtrate was evaporated to dryness to give corresponding *N*-(3-hydroxyphenyl)carbamate. This carbamate was converted to bis(carbamate) by reaction with phenylisocyanate derivative (0.010 mol) in dry benzene (50 mL) in presence of catalytic amount of TEA (few drops) under reflux for 30 min. Solvent was removed under reduced pressure and the residue was purified by column chromatography on silica gel (EtOAc/*n*-hexane (1/2)).

O-3-[(Butoxycarbonyl)amino]phenyl-*N*-(3-methylphenyl)carbamate **5**

White crystalline solid; yield: 63%; mp 115–116 °C; FT-IR (cm^{-1}): υ 3290; 1699; 1538; 1426; 1218; 1042; 778; 688. ^1H NMR (400 MHz, $CDCl_3$): δ 7.36 (bs, 1H, NH), 7.28 (bs, 1H, NH), 7.13 (m, 5H, Ph), 6.87 (m, 3H, Ph), 4.16 (t, ^3J = 6.8 Hz, 2H, OCH_2), 2.32 (s, 3H, CH_3), 1.64 (m, 2H, CH_2), 1.40 (m, 2H, CH_2), 0.94 (t, ^3J = 7.2 Hz, 3H, CH_3); ^{13}C NMR (100 MHz, $CDCl_3$): δ 153.8, 153.5, 151.2, 139.3, 139.2, 137.4, 129.7, 129.1, 128.9, 124.9, 124.3, 121.0, 117.4, 116.6, 65.4, 31.1, 21.6, 19.2, 13.9. HR-MALDI-MS (DHB): calcd for $C_{19}H_{22}N_2O_4$ *m/z* 365.14718 ($[M+Na]^+$), found 365.14736.

O-3-[(Ethoxycarbonyl)amino]phenyl-*N*-(4-methoxyphenyl)carbamate **6**

White crystalline solid; yield: 59%; mp 160–161 °C; FT-IR (cm^{-1}): υ 3324; 1709; 1534; 1435; 1220; 1022; 865; 644. ^1H NMR (400 MHz, DMSO-d_6): δ 10.05 (bs, 1H, NH), 9.80 (bs, 1H, NH), 7.43 (m, 3H, Ph), 7.32 (m, 2H, Ph), 6.92 (m, 2H, Ph), 6.85 (m, 1H, Ph), 4.13 (q, ^3J = 7.2 Hz, 2H, OCH_2), 3.71 (s, 3H, OCH_3), 1.24 (t, ^3J = 7.2 Hz, 3H, CH_3); ^{13}C NMR (100 MHz,

DMSO-d_6): δ 154.8, 153.1, 151.3, 150.5, 139.9, 131.2, 129.0, 119.7, 119.5, 115.3, 114.5, 113.7, 113.5, 111.1, 59.9, 54.7, 14.1. HR-MALDI-MS (DHB): calcd for $C_{19}H_{22}N_2O_5$ *m/z* 353.11080 ($[M+Na]^+$), found 353.11149.

O-3-[(Butoxycarbonyl)amino]phenyl-*N*-(4-methoxyphenyl)carbamate **7**

White crystalline solid; yield: 67%; mp 131–132 °C; FT-IR (cm^{-1}): υ 3329; 1709; 1533; 1432; 1219; 1020; 863; 642. ^{1}H NMR (400 MHz, DMSO-d_6): δ 10.08 (bs, 1H, NH), 9.83 (bs, 1H, NH), 7.39 (m, 3H, Ph), 7.29 (m, 2H, Ph), 6.90 (m, 2H, Ph), 6.83 (m, 1H, Ph), 4.08 (t, ^3J = 6.8 Hz, 2H, OCH_2), 3.72 (s, 3H, OCH_3), 1.60 (m, 2H, CH_2), 1.37 (m, 2H, CH_2), 0.91 (t, ^3J = 7.4 Hz, 3H, CH_3); ^{13}C NMR (100 MHz, DMSO-d_6): δ 155.2, 153.6, 151.7, 150.9, 140.3, 131.6, 129.5, 120.1, 115.7, 115.0, 114.1, 111.6, 64.0, 55.2, 30.6, 18.6, 13.7. HR-MALDI-MS (DHB): calcd for $C_{19}H_{22}N_2O_5$ *m/z* 381.14209 ($[M+Na]^+$), found 381.14222.

O-3-[(Butoxycarbonyl)amino]phenyl-*N*-(3,4-dichlorophenyl)carbamate **12**

White crystalline solid; yield: 71%; mp 137–138 °C; FT-IR (cm^{-1}): υ 3269; 1700; 1591; 1539; 1476; 1214; 1078; 1019; 868; 765; 683; 609.^{1}H NMR (400 MHz, DMSO-d_6): δ 10.57 (bs, 1H, NH), 9.80 (bs, 1H, NH), 7.80 (m, 1H, Ph), 7.59 (m, 1H, Ph), 7.44 (m, 2H, Ph), 7.32 (m, 2H, Ph), 6.88–6.85 (m, 1H, Ph), 4.08 (m, 2H, OCH_2), 1.60 (m, 2H, CH_2), 1.37 (m, 2H, CH_2), 0.91 (t, ^3J = 7.6 Hz, 3H, CH_3); ^{13}C NMR (100 MHz, DMSO-d_6): δ 153.6, 151.5, 150.5, 140.4, 138.9, 131.2, 130.9, 129.5, 124.5, 119.6, 118.5, 115.6, 115.3, 111.4, 64.0, 30.6, 18.6, 13.6. HR-MALDI-MS (DHB): calcd for $C_{18}H_{18}Cl_2N_2O_4$ *m/z* 419.05358 ($[M+Na]^+$), found 419.05435.

*4.1.2.2 Synthesis of O-glycosyl-N-(3,4-dichlorophenyl) and O-glycosyl-N-(3-trifluorophenyl) carbamates **13-18***

To the solution of substituted phenylisocyanate (1.33 mmol) in dry 1,4-dioxane (5 mL) was added corresponding protected monosaccharide (1.60 mmol) and TEA (1.60 mmol). The mixture was heated to reflux for 72 h, and then, the solvent was removed under reduced pressure. The crude products were purified by column chromatography on silica gel (EtOAc/*n*-hexane (1/1)).

O-(1,2:3,4-Di-*O*-isopropylidene-*α*-D-galactopyranose-6-yl)-*N*-(3,4-dichlorophenyl)carbamate **13**

White crystalline solid; yield: 67%; mp 63–65 °C; FT-IR (cm^{-1}): υ 3314; 2987; 1761; 1592; 1523; 1478; 1380; 1210; 1116; 1003; 894; 689; 511. ^{1}H NMR (400 MHz, $CDCl_3$): δ 7.61 (s, 1H, Ph), 7.34 (d, ^3J = 8.8 Hz, 1H, Ph), 7.19 (dd, ^3J = 8.8, 2.8 Hz, 1H, Ph), 6.89 (bs, 1H, NH),

5.57 (m, 1H, CH), 4.64 (m, 1H, CH), 4.37 (m, 2H, 2xCH), 4.28 (m, 2H, OCH_2), 4.08 (m, 1H, CH), 1.52 (s, 3H, CH_3), 1.47 (s, 3H, CH_3), 1.36 (s, 3H, CH_3), 1.34 (s, 3H, CH_3); ^{13}C NMR (100 MHz, $CDCl_3$): δ 153.1, 137.6, 133.1, 130.7, 126.8, 120.4, 118.0, 110.0, 109.1, 96.5, 71.3, 70.9, 70.5, 66.4, 64.9, 26.2, 26.2, 25.1, 24.7. HR-MALDI-MS (DHB): calcd for $C_{19}H_{23}Cl_2NO_7$ *m/z* 470.07438 ($[M+Na]^+$), found 470.07551.

O-(1,2:3,4-Di-*O*-isopropylidene-*α*-D-galactopyranose-6-yl)-*N*-(3-(trifluoromethyl)phenyl)carbamate **14**

White crystalline solid; yield: 66%; mp 51–53 °C; FT-IR (cm^{-1}): υ 3321; 2988; 1717; 1550; 1335; 1210; 1066; 1000; 891; 765; 698; 510.^{1}H NMR (400 MHz, $CDCl_3$): δ 7.68 (bs, 1H, NH), 7.52 (m, 1H, Ph), 7.35 (m, 1H, Ph), 7.25 (s, 2H, Ph), 5.53 (m, 1H, CH), 4.60 (m, 1H, CH), 4.37 (m, 1H, CH), 4.33 (m, 1H, CH), 4.25 (m, 2H, OCH_2), 4.08 (m, 1H, CH), 1.48 (s, 3H, CH_3), 1.42 (s, 3H, CH_3), 1.31 (s, 3H, CH_3), 1.29 (s, 3H, CH_3); ^{13}C NMR (100 MHz, $CDCl_3$): δ 153.4, 138.7, 132.0, 131.7, 131.4, 131.0, 129.7, 128.1, 125.4, 122.7, 121.8, 120.1, 120.0, 115.5, 109.9, 109.0, 96.5, 71.2, 70.9, 70.5, 66.4, 64.7, 26.1, 26.1, 25.0, 24.6. HR-MALDI-MS (DHB): calcd for $C_{20}H_{24}F_3NO_7$ *m/z* 470.13971 ($[M+Na]^+$), found 470.14033.

O-(1,2:5,6-Di-*O*-isopropylidene-α-D-glucofuranose-3-yl)-*N*-(3,4-dichlorophenyl)carbamate **15**

White crystalline solid; yield: 65%; mp 102–104 °C; FT-IR (cm^{-1}): υ 3298; 2988; 1737; 1593; 1529; 1471; 1383; 1210; 1054; 1019; 875; 670. ^{1}H NMR (400 MHz, $CDCl_3$): δ 7.61 (s, 1H, Ph), 7.35 (d, ^3J = 8.8 Hz, 1H, Ph), 7.18 (dd, ^3J = 8.8, 2.8 Hz, 1H, Ph), 7.04 (bs, 1H, NH), 5.88 (m, 1H, CH), 5.24 (m, 1H, CH), 4.63 (m, 1H, CH), 4.27 (m, 1H, CH), 4.21 (m, 1H, CH), 4.05 (m, 2H, OCH_2), 1.53 (s, 3H, CH_3), 1.43 (s, 3H, CH_3), 1.32 (s, 3H, CH_3), 1.31 (s, 3H, CH_3); ^{13}C NMR (100 MHz, $CDCl_3$): δ 151.8, 137.2, 133.1, 130.7, 127.1, 120.3, 117.9, 112.7, 110.0, 105.1, 83.5, 79.8, 77.6, 72.5, 67.6, 27.1, 26.9, 26.3, 25.4. HR-MALDI-MS (DHB): calcd for $C_{19}H_{23}Cl_2NO_7$ *m/z* 470.07438 ($[M+Na]^+$), found 470.07499.

O-(1,2:5,6-Di-*O*-isopropylidene-α-D-glucofuranose-3-yl)-*N*-(3-(trifluoromethyl)phenyl)carbamate **16**

White crystalline solid; yield: 44%; mp 51–53 °C; ; FT-IR (cm^{-1}): υ 3314; 2988; 1742; 1551; 1334; 1207; 1068; 1017; 838; 698. ^{1}H NMR (400 MHz, $CDCl_3$): δ 7.69 (bs, 1H, NH), 7.54 (m, 1H, Ph), 7.36 (m, 3H, Ph), 5.90 (m, 1H, CH), 5.29 (m, 1H, CH), 4.66 (m, 1H, CH), 4.35 (m, 1H, CH), 4.25 (m, 1H, CH), 4.11 (m, 2H, OCH_2), 1.55 (s, 3H, CH_3), 1.45 (s, 3H, CH_3), 1.34 (s, 3H, CH_3), 1.32 (s, 3H, CH_3); ^{13}C NMR (100 MHz, $CDCl_3$): δ 151.9, 138.3, 132.2, 131.8, 131.5, 131.2, 129.8, 128.0, 125.3, 122.6, 121.6, 120.5, 120.5, 115.3, 112.7, 110.0,

105.2, 83.6, 79.9, 77.4, 72.5, 67.6, 27.1, 26.9, 26.3, 25.4. HR-MALDI-MS (DHB): calcd for $C_{20}H_{24}F_3NO_7$ *m/z* 470.13971 ($[M+Na]^+$), found 470.14062.

O-(2,3:4,5-Di-*O*-isopropylidene-*β*-D-fructopyranose-1-yl)-*N*-(3,4-dichlorophenyl)carbamate **17**

White crystalline solid; yield: 57%; mp 163–165 °C; FT-IR (cm^{-1}): υ 3411; 2998; 1729; 1510; 1380; 1209; 1068; 870; 579. ^{1}H NMR (400 MHz, $CDCl_3$): *δ* 7.60 (s, 1H, Ph), 7.32 (d, ^3J = 8.8 Hz, 1H, Ph), 7.18 (dd, ^3J = 8.8, 2.8 Hz, 1H, Ph), 6.83 (bs, 1H, NH), 4.59 (m, 1H, CH), 4.48 (m, 1H, CH), 4.27 (m, 1H, CH), 4.30 (m, 1H, CH), 4.17 (m, 1H, CH), 3.88 (m, 1H, OCH_2), 3.77 (m, 1H, OCH_2), 1.53 (s, 3H, CH_3), 1.48 (s, 3H, CH_3), 1.37 (s, 3H, CH_3), 1.33 (s, 3H, CH_3); ^{13}C NMR (100 MHz, $CDCl_3$): *δ* 152.7, 137.3, 133.1, 130.7, 127.0, 120.5, 118.1, 109.3, 109.0, 101.6, 71.1, 70.8, 70.2, 67.1, 61.5, 26.5, 26.1, 25.3, 24.2. HR-MALDI-MS (DHB): calcd for $C_{19}H_{23}Cl_2NO_7$ *m/z* 470.07438 ($[M+Na]^+$), found 470.07514.

O-(2,3:4,5-Di-*O*-isopropylidene-*β*-D-fructopyranose-1-yl)-*N*-(3-(trifluoromethyl)phenyl)carbamate **18**

White crystalline solid; yield: 31%; mp 47–49 °C; FT-IR (cm^{-1}): υ 3350; 2986; 1744; 1533; 1448; 1220; 1182; 1068; 1047; 883; 696.^{1}H NMR (400 MHz, $CDCl_3$): *δ* 7.73 (bs, 1H, NH), 7.58 (m, 1H, Ph), 7.41 (m, 1H, Ph), 7.30 (m, 2H, Ph), 4.62 (m, 1H, CH), 4.54 (m, 1H, CH), 4.33 (m, 1H, CH), 4.26 (m, 1H, CH), 4.20 (m, 1H, CH), 3.92 (m, 1H, OCH_2), 3.79 (m, 1H, OCH_2), 1.55 (s, 3H, CH_3), 1.50 (s, 3H, CH_3), 1.40 (s, 3H, CH_3), 1.35 (s, 3H, CH_3); ^{13}C NMR (100 MHz, $CDCl_3$): *δ* 152.9, 138.6, 132.0, 131.7, 131.4, 131.1, 129.7, 128.0, 125.3, 122.6, 121.9, 120.2, 119.9, 115.6, 109.3, 108.9, 101.7, 71.0, 70.8, 70.1, 66.7, 60.6, 26.5, 26.0, 25.2, 24.1. HR-MALDI-MS (DHB): calcd for $C_{20}H_{24}F_3NO_7$ *m/z* 470.13971 ($[M+Na]^+$), found 470.14036.

*4.1.2.3 General procedure for deprotection of carbamates **13-18***

The solution of carbamate **13-18** (0.5 mmol) in the mixture of H_2O/TFA (1/1; v/v; 5 mL) was stirred at room temperature for 24 h. The solvents were removed under reduced pressure and the residue was dissolved in MeOH (10 mL) and the solvent was distilled off. This procedure was repeated at least fivefold. The crude products were purified by column chromatography on silica gel (CH_2Cl_2/MeOH (1/1)).

O-(*α*/*β*-D-Galactopyranose-6-yl)-*N*-(3,4-dichlorophenyl)carbamate **19**

White crystalline solid; yield: 83%; decomposition 117–120 °C; FT-IR (cm^{-1}): υ 3291; 1669; 1595; 1524; 1201; 1134; 1075; 1047; 1017; 801; 516. ^{1}H NMR (400 MHz, CD_3OD): δ 7.68 (m, 2H, Ph), 7.33 (m, 2H, Ph), 7.26 (m, 2H, Ph), 5.13 (m, 1H, CH), 4.43 (m, 1H, CH), 4.26 (m, 5H, 5xCH), 3.90 (m, 1H, CH), 3.83 (m, 1H, CH), 3.76 (m, 2H, OCH_2), 3.47 (m, 2H, OCH_2), 3.27 (m, 1H, CH); ^{13}C NMR (100 MHz, CD_3OD): δ 155.3, 155.3, 140.3, 133.3, 131.5, 126.6, 120.9, 119.2, 98.6, 94.2, 74.7, 74.1, 73.6, 71.0, 70.3, 70.2, 69.7, 69.4, 65.6, 65.4. HR-MALDI-MS (DHB): calcd for $C_{13}H_{15}Cl_2NO_7$ *m/z* 390.01178 ($[M+Na]^+$), found 390.01254.

O-(*α*/*β*-D-Galactopyranose-6-yl)-*N*-(3-(trifluoromethyl)phenyl)carbamate **20**

White crystalline solid; yield: 85%; decomposition 109–112 °C; FT-IR (cm^{-1}): υ 3303; 1670; 1548; 1453; 1335; 1202; 1100; 1067; 696; 519. ^{1}H NMR (400 MHz, CD_3OD): δ 7.81 (s, 2H, Ph), 7.57 (d, ^{3}J = 8.0 Hz, 2H, Ph), 7.40 (t, ^{3}J = 8.0 Hz, 2H, Ph), 7.24 (d, ^{3}J = 8.0 Hz, 2H, Ph), 5.16 (m, 1H, CH), 4.46 (m, 1H, CH), 4.27 (m, 5H, 5xCH), 3.93 (m, 1H, CH), 3.87 (m, 1H, CH), 3.79 (m, 2H, OCH_2), 3.49 (m, 2H, OCH_2); ^{13}C NMR (100 MHz, CD_3OD): δ 155.5, 155.5, 141.0, 132.6, 132.3, 131.9, 131.6, 130.6, 129.5, 126.8, 124.1, 122.8, 121.4, 120.2, 115.9, 98.6, 94.1, 74.7, 74.1, 73.6, 71.0, 70.9, 70.3, 70.2, 69.4, 65.5, 65.4. HR-MALDI-MS (DHB): calcd for $C_{14}H_{16}F_3NO_7$ *m/z* 390.07711 ($[M+Na]^+$), found 390.07790.

O-(*α*/*β*-Glucopyranose-3-yl)-*N*-(3,4-dichlorophenyl)carbamate **21**

White crystalline solid; yield: 97%; decomposition 167–170 °C; FT-IR (cm^{-1}): υ 3277; 1677; 1535; 1247; 1113; 1097; 1027; 561. ^{1}H NMR (400 MHz, CD_3OD): δ 7.72 (m, 2H, Ph), 7.31 (m, 4H, Ph), 5.11 (m, 2H, 2xCH), 4.56 (m, 1H, CH), 3.86–3.63 (m, 5H, 5xCH), 3.50 (m, 3H, 1xOCH_2, CH), 3.36 (m, 1H, CH), 3.27 (m, 2H, OCH_2); ^{13}C NMR (100 MHz, CD_3OD): δ 155.8, 155.5, 140.5, 133.3, 131.4, 126.4, 121.0, 119.3, 98.1, 93.9, 80.0, 78.0, 77.8, 74.7, 72.9, 72.2, 69.9, 69.8, 62.5, 62.3. HR-MALDI-MS (DHB): calcd for $C_{13}H_{15}Cl_2NO_7$ *m/z* 390.01178 ($[M+Na]^+$), found 390.01259.

O-(*α*/*β*-D-Glucopyranose-3-yl)-*N*-(3-(trifluoromethyl)phenyl)carbamate **22**

White crystalline solid; yield: 67%; decomposition 125–128 °C; FT-IR (cm^{-1}): υ 3296; 1679; 1544; 1332; 1240; 1116; 1017; 725. ^{1}H NMR (400 MHz, CD_3OD): δ 7.84 (s, 2H, Ph), 7.60 (d, ^{3}J = 8.0 Hz, 2H, Ph), 7.39 (t, ^{3}J = 8.0 Hz, 2H, Ph), 7.23 (d, ^{3}J = 8.0 Hz, 2H, Ph), 5.16 (m, 1H, 1xCH), 5.12 (m, 1H, 1xCH), 4.60 (m, 1H, CH), 3.90–3,67 (m, 5H, 5xCH), 3.56 (m, 3H, 1xOCH_2, CH), 3.35 (m, 3H,1xOCH_2, CH); ^{13}C NMR (100 MHz, CD_3OD): δ 156.0, 155.8, 141.1, 132.5, 132.2, 131.9, 131.5, 130.5, 129.5, 126.8, 124.1, 122.9, 121.4, 120.1 116.0, 98.1,

93.9, 80.0, 77.9, 77.7, 74.6, 72.9, 72.1, 69.9, 69.7, 62.4, 62.2. HR-MALDI-MS (DHB): calcd for $C_{14}H_{16}F_3NO_7$ *m/z* 390.07711 ($[M+Na]^+$), found 390.07787.

O-(*α*/*β*-D-Fructofuranose-1-yl)-*N*-(3,4-dichlorophenyl)carbamate **23**

White crystalline solid; yield: 89%; decomposition 171–173 °C; FT-IR (cm^{-1}): υ 3278; 1715; 1592; 1538; 1226; 1115; 1067; 785; 417. ^{1}H NMR (400 MHz, CD_3OD): *δ* 7.74 (m, 2H, Ph), 7.38 (m, 2H, Ph), 7.31 (m, 2H, Ph), 4.27–4.02 (m, 7H, 5xCH, OCH_2), 3.88 (m, 1H, OCH_2), 3.83 (m, 1H, OCH_2), 3.75 (m, 3H, CH, CH_2), 3.65 (m, 2H, CH_2); ^{13}C NMR (100 MHz, CD_3OD): *δ* 155.2, 155.2, 140.3, 133.3, 131.5, 126.6, 120.9, 119.2, 101.6, 98.3, 83.3, 78.3, 76.4, 71.4, 71.0, 69.5, 67.1, 66.1, 64.7, 64.1. HR-MALDI-MS (DHB): calcd for $C_{13}H_{15}Cl_2NO_7$ *m/z* 390.01178 ($[M+Na]^+$), found 390.01244.

O-(*α*/*β*-D-Fructofuranose-1-yl)-*N*-(3-(trifluoromethyl)phenyl)carbamate **24**

White crystalline solid; yield: 67%; decomposition 151–153 °C; FT-IR (cm^{-1}): υ 3274; 1718; 1565; 1336; 1229; 1094; 1067; 761; 522. ^{1}H NMR (400 MHz, CD_3OD): *δ* 7.86 (s, 2H, Ph), 7.63 (m, 2H, Ph), 7.46 (t, ^3J = 8.0 Hz, 2H, Ph), 7.29 (d, ^3J = 8.0 Hz, 2H, Ph), 4.28–4.02 (m, 7H, 5xCH, OCH_2), 3.88 (m, 1H, OCH_2), 3.83 (m, 1H, CH, OCH_2), 3.75 (m, 3H, CH, CH_2), 3.64 (m, 2H, CH_2); ^{13}C NMR (100 MHz, CD_3OD): *δ* 155.4, 155.2, 141.2, 132.7, 132.3, 132.0, 131.7, 130.7, 129.6, 126.9, 124.2, 122.8, 121.6, 120.2, 115.9, 101.6, 98.3, 83.4, 78.4, 76.4, 71.4, 71.0, 69.6, 67.1, 66.1, 64.7, 64.2. HR-MALDI-MS (DHB): calcd for $C_{14}H_{16}F_3NO_7$ *m/z* 390.07711 ($[M+Na]^+$), found 390.07797.

4.2 Biology

4.2.1 Determination of actual enzyme activity

For determination of enzyme actual activity modified spectrophotometric Ellman's method (ELM) was used. Ellman's method is a simple, rapid and direct method to determine the SH and -S-S- groups contained in proteins [49]. Cholinesterase activity is measured indirectly by quantifying the concentration of 5-thio-2-nitrobenzoic acid (TNB) ion formed in the reaction between the thiol reagent 5,5′-dithiobis-2-nitrobenzoic acid and thiocholine (TCh), a product of substrate (i.e. acetylthiocholine, ATCh, or butyrylthiocholine, BTCh) hydrolysis catalyzed by cholinesterase [50].

Cholinesterase activity was determined using ELM at 25 °C in presence of 0.1 mol/L phosphate buffered saline (PBS, pH 7.4) in glass cuvette with 1 cm optical path. Product of given enzymatic reaction, TNB, was detected by spectrophotometer with diode array Hewlett-Packard 8453 at the wavelength of 412 nm against comparative solution. The dependence of absorbance A (412 nm) *vs.* time (t) was observed for 70 s and actual activity of enzyme was calculated. Measurement of activity was carried out in triplicate at least. The average value of daily determined catalytic activity of given enzyme was used to calculate its suitable volume which had to be added into initial reaction mixture for determination of inhibitory effect to achieve the final activity in reaction mixture 0.2 U/mL.

4.2.2 Determination of cholinesterase inhibition in presence of substituted N-phenylcarbamates

All tested compounds (Table 1) were dissolved in DMSO to concentration 0.01 M and then diluted in demineralized water as necessary. The inhibitory efficiency of tested substituted *N*-phenylcarbamates was evaluated by the value of IC_{50} (50% inhibitory concentration, i.e. the concentration of inhibitor that is necessary for reduction of enzyme activity or reaction rate to 50%). For determination of IC_{50} the previously published measuring procedure (modified Ellman's method) was used [46]. The enzyme activity in total reaction mixture (2000 μL) was 0.2 U/mL, concentration of ATCh (or BTCh) 40 μM and concentration of DTNB 0.1 mM for all reactions.

For all tested compounds and standards (Rivastigmine and Galanthamine) four or five different concentrations of inhibitor (or standard) were used. Measurements were carried out in duplicate at least, and the average value of reaction rate (v_i) was calculated. Then the dependence v_0/v_i *vs.* concentration of inhibitor was constructed and IC_{50} was calculated from obtained equation of regression curve (based on the definition of IC_{50}).

4.2.3 Investigation of inhibition type

For the determination of the inhibition mechanism a Lineweaver-Burk plot was used [51] and the measuring procedure was similar to that for determination of IC_{50}. Five *N*-phenylcarbamates (**1**, **10**, **12**, **13** and **18**: see Table 1) and four different concentrations of substrate (20, 40, 60 and 80 μM) were used for investigation of cholinesterase inhibitory mechanism. For each of substrate concentration four or five different concentrations of inhibitor were chosen according to their IC_{50} values. Each measurement was performed in duplicate. The dependence of absorbance (412 nm) on time was measured, and the reaction rate was calculated for uninhibited and inhibited reactions. Then, a Lineweaver-Burk plot was constructed, and Michaelis constant and maximum rate were calculated. The purpose was to observe the effect of inhibitor on kinetic parameters.

4.2.4 Determination of partition coefficient in system n-octanol/water

The partition coefficient serves as a quantitative descriptor of lipophilicity and is one of the key determinants of pharmacokinetic properties. The partition coefficient P_{ow} (*n*-octanol/water) indicates potential of the drug for crossing the blood-brain barrier for direct inhibition of brain cholinesterases. The classical and most reliable method of partition coefficient determination is the „shake-flask method“, which consists of dissolving some of the solute in question in volume of *n*-octanol and water, then measuring the concentration of the solute in each solvent [52]. The most common method of measuring the distribution of the solute is by UV/VIS spectroscopy.

In first step, into the test tube 2000 μL of *n*-octanol were placed. Then 15 μL of *n*-octanol solution of chosen inhibitor (0.01 M) were added. Mixture was intensively shaken for 15 min. Then 1000 μL of this mixture was placed into the cuvette and its absorbance at the wavelength of absorption maximum was measured. Comparative solution was *n*-octanol. The

value of absorbance which is corresponding to 100% of chosen inhibitor in *n*-octanol was obtained.

In second step, 15 µL of *n*-octanol solution of chosen inhibitor (0.01 M) were added into the mixture of *n*-octanol (2000 µL) and demineralized water (2000 µL). Mixture was intensively shaken for 15 min and then centrifuged (3000 rpm, 10 min). Consequently, 1000 µL of the *n*-octanol layer was put into the cuvette and its absorbance at the wavelength of absorption maximum was measured. Comparative solution was *n*-octanol again. Percentage content of chosen inhibitor in the *n*-octanol layer $(\%)_1$ was obtained. Then the percentage content of inhibitor in the water layer was calculated [100 - $(\%)_1$]. Partition coefficients were calculated according to eq. 1, where c_1 and c_2 are molar concentrations of the chosen inhibitor in *n*-octanol and water.

$$P_{ow} = \frac{c_1}{c_2} \quad (1)$$

4.2.5 Molecular modeling of ligand-enzyme interaction

The starting structures of compounds **1-24** were obtained by equilibrium conformer systematic search (MMFF94) in the program SPARTAN'08 (Wavefunction, Inc., Irvine, CA, 2009). The crystallographic structures of human enzymes were taken from the Brookhaven protein databank: the structure with pdb code 4m0f for AChE and 5k5e for BChE. The protonation state corresponding to the experimental pH 7.4 was taken into account. The standard docking protocol and YAMBER3 force field included in program YASARA were used. The maximum number of the first five clusters was then searched for the minimum value of the binding energy E_{bin} within the optimization protocol em_run.mcr, which allows optimizing the whole complex by a combination of gradient optimization, simulated annealing and single molecular dynamics calculation in water. The optimal geometries of the complexes were then used for analysing the key interactions.

Declaration of interest

The authors declare no conflict of interest.

Acknowledgements

This work was supported by the Faculty of Chemical Technology, University of Pardubice and VEGA 2/0033/14.

References

[1] I. Yanovsky, E. Finkin-Groner, A. Zaikin, L. Lerman, H. Shalom, S. Zeeli, T. Weill, I. Ginsburg, A. Nudelman, M. Weinstock, Carbamate derivatives of indolines as cholinesterase inhibitors and antioxidants for the treatment of Alzheimer's disease, J. Med. Chem. 55 (2012) 10700–10715. doi:10.1021/jm301411g.

[2] M. Krátký, Š. Štěpánková, K. Vorčáková, J. Vinšová, Salicylanilide diethyl phosphates as cholinesterases inhibitors., Bioorg. Chem. 58 (2015) 48–52. doi:10.1016/j.bioorg.2014.11.005.

[3] S.Y. Chiou, C.F. Huang, M.T. Hwang, G. Lin, Comparison of active sites of butyrylcholinesterase and acetylcholinesterase based on inhibition by geometric isomers of benzene-di-N-substituted carbamates, J. Biochem. Mol. Toxicol. 23 (2009) 303–308. doi:10.1002/jbt.20286.

[4] Š. Štěpánková, K. Komers, Cholinesterases and Cholinesterase Inhibitors, Curr. Enzym. Inhib. 4 (2008) 160–171. doi:10.2174/157340808786733631.

[5] P. Anand, B. Singh, A review on cholinesterase inhibitors for Alzheimer's disease, Arch. Pharm. Res. 36 (2013) 375–399. doi:10.1007/s12272-013-0036-3.

[6] C. Bartolucci, J. Stojan, Q. Yu, N.H. Greig, D. Lamba, Kinetics of Torpedo californica acetylcholinesterase inhibition by bisnorcymserine and crystal structure of the complex with its leaving group, Biochem. J. 444 (2012) 269–277. doi:10.1042/BJ20111675.

[7] Q. Yu, H.W. Holloway, T. Utsuki, A. Brossi, N.H. Greig, N. Carolina, Synthesis of Novel Phenserine-Based-Selective Inhibitors of Butyrylcholinesterase for Alzheimer ' s Disease †, (1999) 1855–1861.

[8] A.K. Ghosh, M. Brindisi, Organic Carbamates in Drug Design and Medicinal Chemistry, (2015). doi:10.1021/jm501371s.

[9] W.K. Anderson, A.S. Milowsky, 3-Pyrroline N-oxide bis(carbamate) tumor inhibitors as analogues of indicine N-oxide., J. Med. Chem. 30 (1987) 2144–7. http://www.ncbi.nlm.nih.gov/pubmed/3669020 (accessed March 9, 2018).

[10] W.K. Anderson, R.H. Mach, Synthesis and chemical reactivity of c-5 substituted 6,7-bis-(hydroxymethyl)-1 *H* -pyrrolizine biscarbamate tumor inhibitors, J. Heterocycl. Chem. 27 (1990) 1025–1030. doi:10.1002/jhet.5570270440.

[11] C.-C. Yu, C.W. Kearns, R.L. Metcalf, J.D. Davies, Acetylcholinesterase inhibition by bis-carbamates, Pestic. Biochem. Physiol. 1 (1971) 241–247. doi:10.1016/0048-3575(71)90201-X.

[12] A. Bosak, I.G. Smilović, A. Štimac, V. Vinković, G. Šinko, Z. Kovarik, Peripheral site and acyl pocket define selective inhibition of mouse butyrylcholinesterase by two biscarbamates, Arch. Biochem. Biophys. 529 (2013) 140–145. doi:10.1016/j.abb.2012.11.012.

[13] A. Bosak, I.G. Smilović, G. Šinko, V. Vinković, Z. Kovarik, Metaproterenol, isoproterenol, and their bisdimethylcarbamate derivatives as human cholinesterase inhibitors, J. Med. Chem. 55 (2012) 6716–6723. doi:10.1021/jm300289k.

[14] L.A. Hardegger, B. Kuhn, B. Spinnler, L. Anselm, R. Ecabert, M. Stihle, B. Gsell, R. Thoma, J. Diez, J. Benz, J.-M. Plancher, G. Hartmann, D.W. Banner, W. Haap, F. Diederich, Systematic Investigation of Halogen Bonding in Protein-Ligand Interactions, Angew. Chemie Int. Ed. 50 (2011) 314–318. doi:10.1002/anie.201006781.

[15] K.E. Riley, P. Hobza, Strength and Character of Halogen Bonds in Protein–Ligand Complexes, Cryst. Growth Des. 11 (2011) 4272–4278. doi:10.1021/cg200882f.

[16] P. Zhou, J. Huang, F. Tian, Specific Noncovalent Interactions at Protein-Ligand Interface: Implications for Rational Drug Design, Curr. Med. Chem. 19 (2012) 226–238. doi:10.2174/092986712803414150.

[17] Y. Lu, Y. Liu, Z. Xu, H. Li, H. Liu, W. Zhu, Halogen bonding for rational drug design and new drug discovery, Expert Opin. Drug Discov. 7 (2012) 375–383. doi:10.1517/17460441.2012.678829.

[18] M.R. Scholfield, C.M. Vander Zanden, M. Carter, P.S. Ho, Halogen bonding (X-bonding): a biological perspective., Protein Sci. 22 (2013) 139–52. doi:10.1002/pro.2201.

[19] R. Wilcken, M.O. Zimmermann, A. Lange, A.C. Joerger, F.M. Boeckler, Principles and Applications of Halogen Bonding in Medicinal Chemistry and Chemical Biology, (2013).

[20] S. Sirimulla, J.B. Bailey, R. Vegesna, M. Narayan, Halogen Interactions in Protein–Ligand Complexes: Implications of Halogen Bonding for Rational Drug Design, J. Chem. Inf. Model. 53 (2013) 2781–2791. doi:10.1021/ci400257k.

[21] Z. Xu, Z. Yang, Y. Liu, Y. Lu, K. Chen, W. Zhu, Halogen Bond: Its Role beyond Drug–Target Binding Affinity for Drug Discovery and Development, J. Chem. Inf. Model. 54 (2014) 69–78. doi:10.1021/ci400539q.

[22] E. Persch, O. Dumele, F. Diederich, Molecular Recognition in Chemical and Biological Systems, Angew. Chemie Int. Ed. 54 (2015) 3290–3327. doi:10.1002/anie.201408487.

[23] G. Cavallo, P. Metrangolo, R. Milani, T. Pilati, A. Priimagi, G. Resnati, G. Terraneo, The Halogen Bond, Chem. Rev. 116 (2016) 2478–2601. doi:10.1021/acs.chemrev.5b00484.

[24] S. Jiang, L. Zhang, D. Cui, Z. Yao, B. Gao, J. Lin, D. Wei, The Important Role of Halogen Bond in Substrate Selectivity of Enzymatic Catalysis, Sci. Rep. 6 (2016) 34750. doi:10.1038/srep34750.

[25] P. Politzer, S. Murray, T. Clark, Halogen bonding : an electrostatically-driven highly directional noncovalent interaction, (2010) 7748–7757. doi:10.1039/c004189k.

[26] Y. Lu, T. Shi, Y. Wang, H. Yang, X. Yan, X. Luo, H. Jiang, W. Zhu, Halogen Bonding s A Novel Interaction for Rational Drug Design ?, (2009) 2854–2862.

[27] P. Politzer, P. Lane, M.C. Concha, Y. Ma, J.S. Murray, An overview of halogen bonding, (2007) 305–311. doi:10.1007/s00894-006-0154-7.

[28] H.G. Bonacorso, A. Ketzer, F.D. Garcia, W.C. Rosa, T.P. Calheiro, S.C. Feitosa, G.M. Dal Forno, N. Zanatta, M.A.P. Martins, C.P. Frizzo, Efficient approach for regioselective synthesis of new trifluoromethyl-substituted spirotetracyclic isoxazolines and isoxazoles, J. Fluor. Chem. 197 (2017) 6–14. doi:10.1016/j.jfluchem.2017.02.004.

[29] Roche - Lariam, (n.d.). http://www.roche.com/products/product-details.htm?productId=9cb37a0c-a786-42ff-a644-d227b644bb34 (accessed May 10, 2017).

[30] M.A.P. Martins, P. Machado, L.A. Piovesan, A.F.C. Flores, M.M.A. de Campos, C. Scheidt, H.G. Bonacorso, N. Zanatta, Microwave-assisted synthesis and antimicrobial activity of 5-trihalomethyl-3-arylisoxazoles, Monatshefte Für Chemie - Chem. Mon. 139 (2008) 985–990. doi:10.1007/s00706-007-0849-1.

[31] K.N. Allen, R.H. Abeles, Inhibition kinetics of acetylcholinesterase with fluoromethyl ketones., Biochemistry. 28 (1989) 8466–73. doi:10.1021/BI00447A029.

[32] U. Brodbeck, K. Schweikert, R. Gentinetta, M. Rottenberg, Fluorinated aldehydes and ketones acting as quasi-substrate inhibitors of acetylcholinesterase, Biochim. Biophys. Acta - Enzymol. 567 (1979) 357–369. doi:10.1016/0005-2744(79)90122-0.

[33] C. Fernández, O. Nieto, A. Fontenla, E. Rivas, M.L. De Ceballos, A. Fernández-mayoralas, Synthesis of glycosyl derivatives as dopamine prodrugs : interaction with glucose carrier GLUT-1 †, (2003) 767–771.

[34] E.C. Calvaresi, P.J. Hergenrother, Glucose conjugation for the specific targeting and treatment of cancer., Chem. Sci. 4 (2013) 2319–2333. doi:10.1039/C3SC22205E.

[35] C. Uriel, M. Egron, M. Santarromana, D. Scherman, K. Antonakis, J. Herscovicp, Hexose Keto-C-glycoside Conjugates : Design , Synthesis , Cytotoxicity , and Evaluation of Their Affinity for the Glucose Transporter Glut-1, 4 (1996) 2081–2090.

[36] H.-G. Joost, B. Thorens, The extended GLUT-family of sugar/polyol transport facilitators: nomenclature, sequence characteristics, and potential function of its novel members, Mol. Membr. Biol. 18 (2001) 247–256. doi:10.1080/09687680110090456.

[37] S. Picard, P. Bouyssou, J. Chenault, Hemisynthesis of the naturally occurring tremuloidin, Phytochemistry. 31 (1992) 2909–2910. doi:10.1016/0031-9422(92)83663-J.

[38] E. Horáková, P. Drabina, L. Brůčková, Š. Štěpánková, K. Vorčáková, M. Sedlák, Synthesis and in vitro evaluation of novel N-cycloalkylcarbamates as potential cholinesterase inhibitors, Monatshefte Fur Chemie. (2017). doi:10.1007/s00706-017-2026-5.

[39] P. Masson, E. Carletti, F. Nachon, Structure, activities and biomedical applications of human butyrylcholinesterase., Protein Pept. Lett. 16 (2009) 1215–1224. doi:10.2174/092986609789071207.

[40] P. Masson, M.T. Froment, S. Fort, F. Ribes, N. Bec, C. Balny, L.M. Schopfer, Butyrylcholinesterase-catalyzed hydrolysis of N-methylindoxyl acetate: Analysis of volume changes upon reaction and hysteretic behavior, Biochim. Biophys. Acta - Protein Struct. Mol. Enzymol. 1597 (2002) 229–243. doi:10.1016/S0167-

4838(02)00265-0.

[41] F. Nachon, Y. Nicolet, N. Viguié, P. Masson, J.C. Fontecilla-Camps, O. Lockridge, Engineering of a monomeric and low-glycosylated form of human butyrylcholinesterase: Expression, purification, characterization and crystallization, Eur. J. Biochem. 269 (2002) 630–637. doi:10.1046/j.0014-2956.2001.02692.x.

[42] O. Lockridge, L.M. Schopfer, G. Winger, J.H. Woods, Large Scale Purification of Butyrylcholinesterase From Human Plasma Suitable for Injection Into Monkeys; a Potential New Therapeutic for Protection Against Cocaine and Nerve Agent Toxicity, J. Med. Chem. Biol. Radiol. Def. 3 (2005) 1–23. doi:10.1901/jaba.2005.3-nihms5095.

[43] H. Li, L.M. Schopfer, P. Masson, O. Lockridge, Lamellipodin proline rich peptides associated with native plasma butyrylcholinesterase tetramers., Biochem. J. 411 (2008) 425–432. doi:10.1042/BJ20071551.

[44] D. Liang, J.P. Blouet, F. Borrega, S. Bon, J. Massoulié, Respective roles of the catalytic domains and C-terminal tail peptides in the oligomerization and secretory trafficking of human acetylcholinesterase and butyrylcholinesterase, FEBS J. 276 (2009) 94–108. doi:10.1111/j.1742-4658.2008.06756.x.

[45] M. Bergon, N. Ben Hamida, J.-P. Calmon, Isocyanate formation in the decomposition of phenmedipham in aqueous media., J. Agric. Food Chem. 33 (1985) 577–583. doi:10.1021/jf00064a007.

[46] E. Horáková, P. Drabina, B. Brož, Š. Štěpánková, K. Vorčáková, K. Královec, R. Havelek, M. Sedlák, Synthesis, characterization and *in vitro* evaluation of substituted *N* -(2-phenylcyclopropyl)carbamates as acetyl- and butyrylcholinesterase inhibitors, J. Enzyme Inhib. Med. Chem. 31 (2016) 173–179. doi:10.1080/14756366.2016.1212193.

[47] M. Bergon, N. Ben Hamida, J.P. Calmon, Isocyanate formation in the decomposition of phenmedipham in aqueous media, J. Agric. Food Chem. 33 (1985) 577–583. doi:10.1021/jf00064a007.

[48] G. Boroschewski, R. Rusch, F. Arndt, Neth. Pat. Appl. NL-6604363 (1967), 104813, 1967.

[49] S. Ou, K.C. Kwok, Y. Wang, H. Bao, An improved method to determine SH and -S-S-group content in soymilk protein, Food Chem. 88 (2004) 317–320. doi:10.1016/j.foodchem.2004.05.001.

[50] G. Šinko, M. Čalić, A. Bosak, Z. Kovarik, Limitation of the Ellman method: Cholinesterase activity measurement in the presence of oximes, Anal. Biochem. 370 (2007) 223–227. doi:10.1016/j.ab.2007.07.023.

[51] H. Lineweaver, D. Burk, The Determination of Enzyme Dissociation Constants, J. Am. Chem. Soc. 56 (1934) 658–666. doi:10.1021/ja01318a036.

[52] A. Noble, Partition coefficients (n-octanol-water) for pesticides, J. Chromatogr. 642 (1993) 3–14. doi:10.1016/0021-9673(93)80072-G.

Tab. 1 List of tested *N*-phenylcarbamates and their inhibitory activity against eeAChE and eqBChE expressed as IC_{50} (μM) in comparison with standards Rivastigmine and Galanthamine, selectivity and partition coefficient expressed as log P_{ow}.

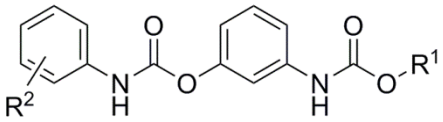

1–12

(*The first group*)

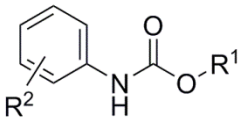

13–24

(*The second group*)

No.	R^1	R^2	IC_{50} (μM)		AChE/BChE ratio	log P_{ow}
			eeAChE	**eqBChE**		
1	Me	-H	20.6 ± 0.3	15.7 ± 1.3	1.3	3.31 ± 0.3
2	Et	-H	12.9 ± 0.2	11.4 ± 0.3	1.1	3.9 ± 0.4
3	*n*Bu	-H	15.7 ± 0.2	11.2 ± 0.6	1.4	5.1 ± 0.7
4	Et	3-Me	18.3 ± 0.4	10.2 ± 0.2	1.8	4.6 ± 0.7
5	*n*Bu	3-Me	20.9 ± 1.0	12.2 ± 0.5	1.7	5.3 ± 0.4
6	Et	4-MeO	15.1 ± 0.7	11.1 ± 0.7	1.4	3.5 ± 0.2
7	*n*Bu	4-MeO	12.4 ± 1.4	12.4 ± 0.4	1.0	5.0 ± 0.5
8	Et	4-Cl	14.1 ± 0.1	22.0 ± 0.2	0.6	4.8 ± 0.5
9	*n*Bu	4-Cl	15.0 ± 0.8	14.5 ±0.4	1.0	5.4 ± 0.6
10	Me	3,4-di(Cl)	7.7 ± 1.2	6.1 ± 0.02	1.3	4.9 ± 0.3
11	Et	3,4-di(Cl)	8.6 ± 0.2	9.6 ± 0.03	0.9	5.3 ± 0.5
12	*n*Bu	3,4-di(Cl)	9.9 ± 0.8	10.5 ± 0.04	0.9	6.3 ± 0.6
13	PG-galactosyl	3,4-di(Cl)	46.9 ± 0.3	29.4 ± 0.03	1.6	6.2 ± 0.6
14	PG-galactosyl	3-CF_3	61. 4 ± 0.8	36.7 ± 0.2	1.7	5.0 ± 0.3
15	PG-glucosyl	3,4-di(Cl)	69.4 ± 1.4	> 200	---	7.3 ± 0.7
16	PG-glucosyl	3-CF_3	70.0 ± 0.9	> 200	---	5.9 ± 0.5
17	PG-fructosyl	3,4-di(Cl)	76.3 ± 2.2	35.3 ± 0.8	2.2	4.9 ± 0.4
18	PG-fructosyl	3-CF_3	76.5 ± 0.03	40.1 ± 0.3	1.9	6.7 ± 0.5
19	Galactosyl	3,4-di(Cl)	94.3 ± 0.1	> 200	---	2.0 ± 0.1
20	Galactosyl	3-CF_3	99.2 ± 2.2	> 200	---	2.03 ± 0.18
21	Glucosyl	3,4-di(Cl)	89.1 ± 2.6	> 200	---	3.1 ± 0.3
22	Glucosyl	3-CF_3	103.4 ± 1.3	> 200	---	1.9 ± 0.1
23	Fructosyl	3,4-di(Cl)	98.0 ± 2.4	> 200	---	3.0 ± 0.4
24	Fructosyl	3-CF_3	103.5 ± 1.0	> 200	---	3.0 ± 0.3
	Rivastigmine		56.1 ± 1.4	66.3 ± 5.3	0.9	2.2 ± 0.2
	Galantamine		1.5 ± 0.02	4.0 ± 0.02	0.4	1.6 ± 0.1

ChE inhibition and partition coefficient are expressed as the mean ± SD (*n* = 2 experiments).

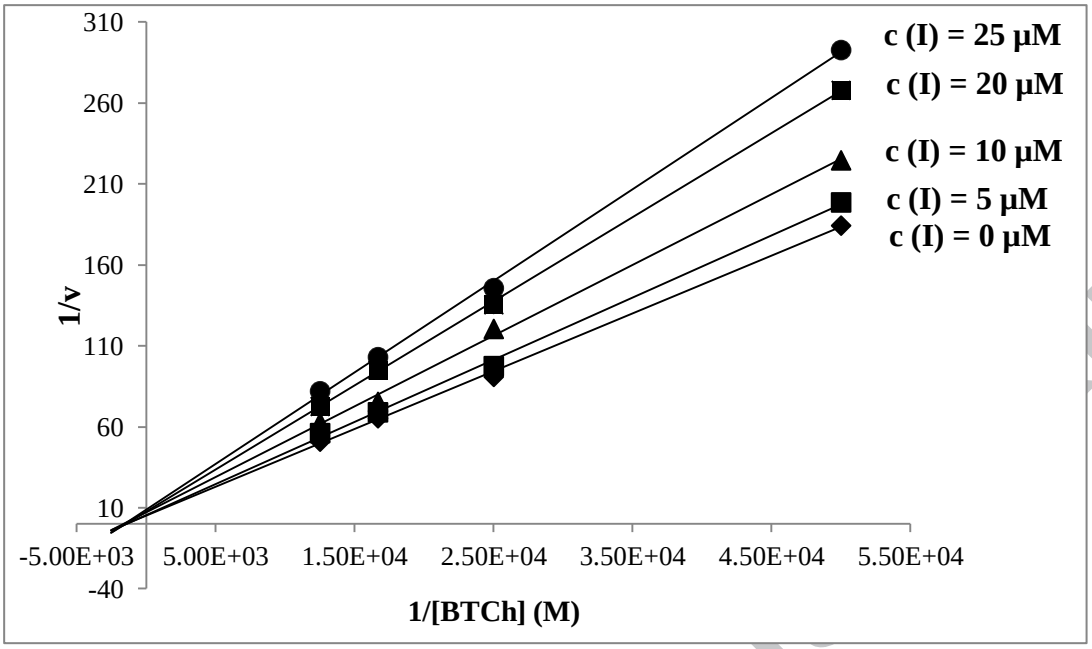

Fig. 1 The example of kinetic analysis of compound **18** for combination BTCh-eqBChE. The measurements were done in duplicate and the points are express as average values.

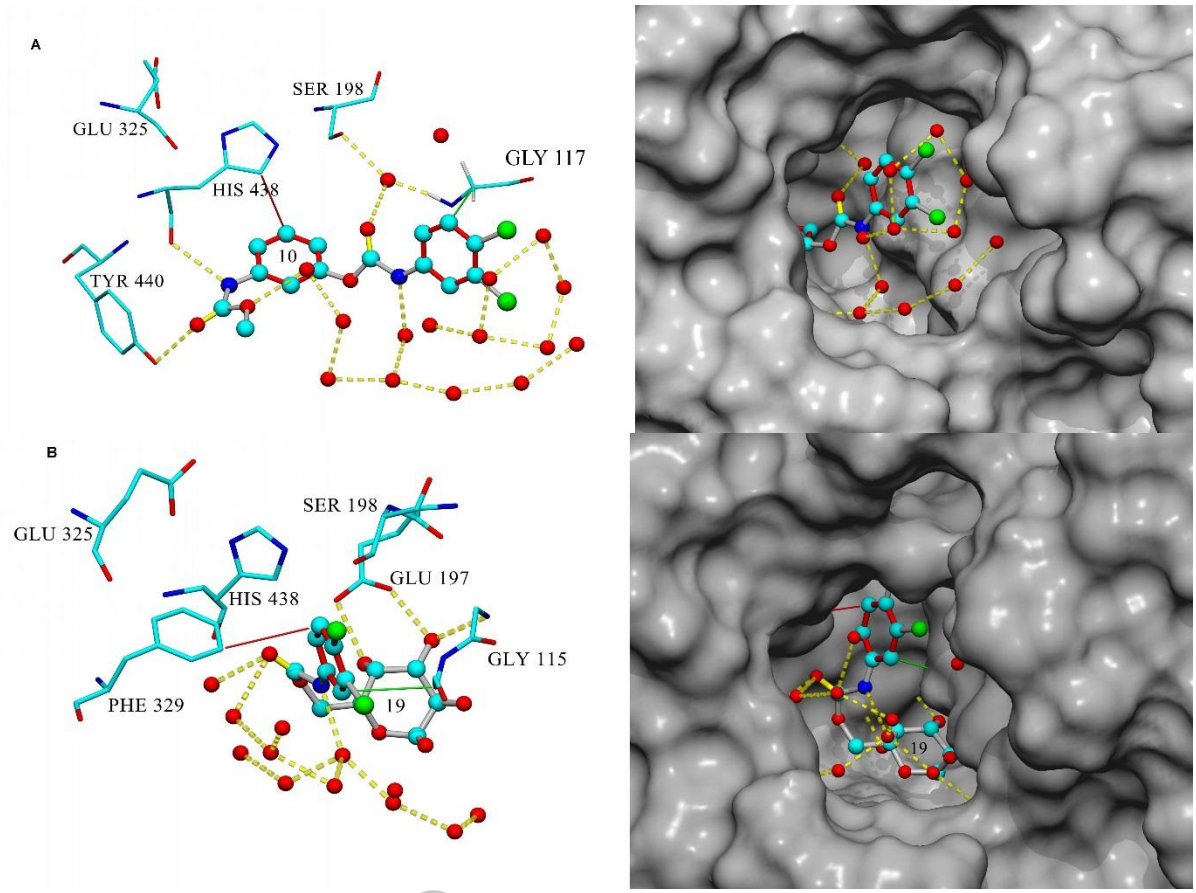

Fig. 2 Molecular modeling for compound **10** (2A) and **19** (2B) in active site of BChE (PDB code: 5k5e).

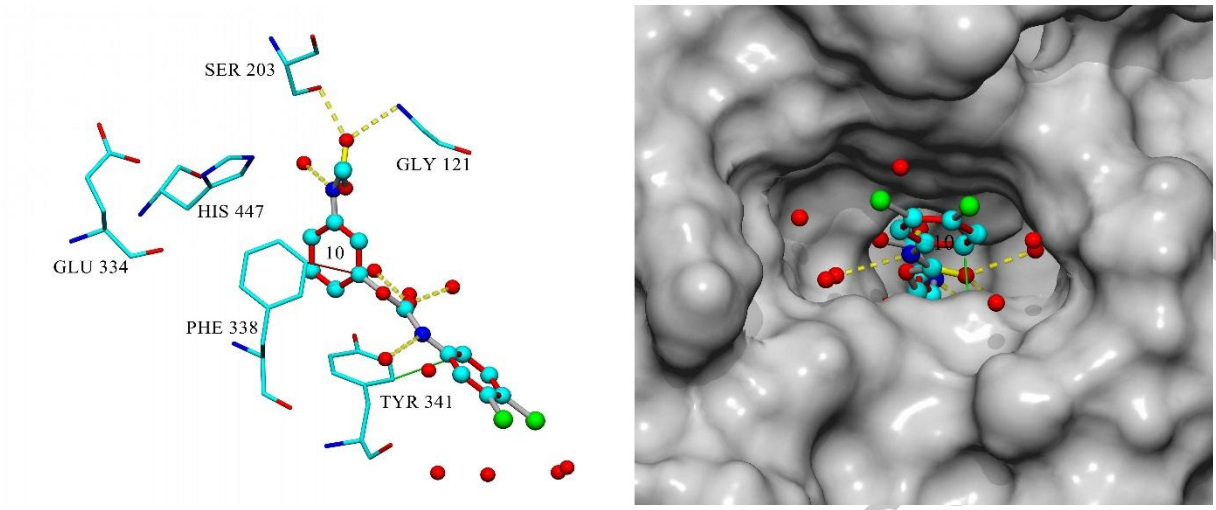

Fig. 3 Molecular modeling for compound **10** in active site of AChE (PDB code: 4m0f).

Highlights:

- Synthesis of *N*-phenylcarbamates with additional carbamate group or with monosaccharide moiety.
- *In vitro* testing of inhibitory effect, type of inhibition and molecular modelling.
- Effect of deacetalization of monosaccharide moiety on inhibitory concentration.
- Importance of phenylcarbamate orientation in the catalytic gorges of cholinesterases.

Graphical abstract